Infection and Drug Resistance

Dovepress
open access to scientific and medical research

Open Access Full Text Article

ORIGINAL RESEARCH

RETRACTED ARTICLE: Functional Study of *desKR*: a Lineage-Specific Two-Component System Positively Regulating *Staphylococcus aureus* Biofilm Formation

Xinyan Ma[1,2,*], Ziyan Wu[1,2,*], Junpeng Li[1,2], Yang Yang[1,2]

[1]College of Veterinary Medicine, Yangzhou University, Yangzhou, 225009, People's Republic of China; [2]Jiangsu Co-Innovation Center for Important Animal Infectious Diseases and Zoonoses, and Joint Laboratory of International Cooperation on Prevention and Control Technology of Important Animal Diseases and Zoonoses of Jiangsu Higher Education Institutions, Yangzhou, 225009, People's Republic of China

*These authors contributed equally to this work

Correspondence: Yang Yang, Email YangyangYZU@163.com

Purpose: Biofilms significantly contribute to the persistence and antibiotic resistance of *Staphylococcus aureus* infections. However, the regulatory mechanisms governing biofilm formation of *S. aureus* remain not fully elucidated. This study aimed to investigate the function of the *S. aureus* lineage-specific two-component system, *desKR*, in biofilm regulation and pathogenicity.

Methods: Bioinformatic analysis was conducted to assess the prevalence of *desKR* across various *S. aureus* lineages and to examine its structural features. The impact of *desKR* on *S. aureus* pathogenicity was evaluated using in vivo mouse models, including skin abscess, bloodstream infection, and nasal colonization models. Crystal violet staining and confocal laser scanning microscopy were utilized to examine the impact of *desKR* on *S. aureus* biofilm formation. Mechanistic insights into *desKR*-mediated biofilm regulation were investigated by quantifying polysaccharide intercellular adhesin (PIA) production, extracellular DNA (eDNA) release, autolysis assays, and RT-qPCR.

Results: The prevalence of *desKR* varied among different *S. aureus* lineages, with notably low carriage rates in ST398 and ST59 lineages. Deletion of *desKR* in NCTC8325 strain resulted in decreased susceptibility to β-lactam and glycopeptide antibiotics. Although *desKR* did not significantly affect acute pathogenicity, the Δ*desKR* mutant exhibited significantly reduced nasal colonization and biofilm-forming ability. Overexpression of *desKR* in naturally *desKR*-lacking strains (ST398 and ST59) enhanced biofilm formation, suggesting a lineage-independent effect. Phenotypic assays further revealed that the Δ*desKR* mutant showed reduced PIA production, decreased eDNA release, and lower autolysis rates. RT-qPCR indicated significant downregulation of *icaA, icaD, icaB*, and *icaC* genes, along with upregulation of *icaR*, whereas autolysis-related genes remained unchanged.

Conclusion: The *desKR* two-component system positively regulates *S. aureus* biofilm formation in a lineage-independent manner, primarily by modulating PIA synthesis via the *ica* operon. These findings provide new insights into the molecular mechanisms of biofilm formation in *S. aureus* and highlight *desKR* as a potential target for therapeutic strategies aimed at combating biofilm-associated infections.

Keywords: *Staphylococcus aureus*, two-component system, *desKR*, biofilm

Introduction

Staphylococcus aureus is a prevalent pathogen responsible for a wide range of infectious diseases, including skin and soft tissue infections, necrotizing pneumonia, and septicemia.[1] The ability of *S. aureus* to form biofilms on various surfaces, including medical devices and host tissues, is a critical factor contributing to its pathogenicity and persistence.[2] Biofilms are complex communities of microorganisms encased in a self-produced extracellular matrix that confers enhanced resistance to antibiotics and host immune defenses.[3] The formation of *S. aureus* biofilms is a multifaceted process involving the coordination of various regulatory systems, especially two-component systems (TCSs).[4,5]

Received: 20 August 2024
Accepted: 9 September 2024
Published: 17 September 2024

TCSs are ubiquitous signaling pathways in bacteria that enable them to sense and respond to environmental stimuli.[6] TCSs typically consist of a histidine kinase (HK) and a response regulator (RR).[7] HKs are generally transmembrane proteins with a highly variable N-terminal sensory domain and a C-terminal domain containing a conserved histidine residue.[8] Upon external signal binding, HKs undergo autophosphorylation and subsequently transfer the phosphate group to the aspartate residue on RRs.[8,9] RRs, usually cytoplasmic proteins, undergo a conformational change upon phosphorylation, activating their effector domains to bind DNA and regulate gene expression.

In *S. aureus*, 16 pairs of TCSs have been identified that play crucial roles in virulence, antimicrobial resistance, and biofilm formation.[5,10] Several TCSs have been implicated in the regulation of *S. aureus* biofilm formation, including *agr, arlRS*, and *saeRS*.[11–13] However, the roles of many other TCSs in *S. aureus* biofilm formation remain largely unexplored. Most TCSs are conserved across the species, contributing to survival and virulence under infectious conditions, making them ideal targets for novel anti-infective strategies.[14,15] However, the function of the seventh TCS pair (TCS-7), homologous to *desK* and *desR* in various bacteria including *Bacillus subtilis*, remains uncharacterized.[16] Given the importance of TCSs in regulating bacterial physiology and virulence, we hypothesized that *desKR* might play a role in *S. aureus* pathogenicity.

To test this hypothesis, we used a combination of bioinformatics, genetic, and phenotypic approaches to investigate the distribution, function, and regulatory mechanisms of *desKR* in *S. aureus*. Our findings provide novel insights into the role of this lineage-specific TCS, which is present in certain *S. aureus* lineages, in biofilm formation and its potential as a target for anti-biofilm strategies. Furthermore, this study highlights the importance of exploring the diversity of regulatory systems in *S. aureus* to better understand the complex mechanisms governing its pathogenicity and adaptation to different niches.

Methods

Bacterial Strains

The strains and plasmids used in this study are listed in Table 1. *S. aureus* NCTC8325 was obtained from the National Collection of Type Culture. Strains SA27 and SA42 were isolated from cows with subclinical mastitis in a herd in Jiangsu province, China. These strains underwent Multi-Locus Sequence Typing (MLST) for seven housekeeping genes (*arcC, aroE, glpF, gmk, pta, tpi*, and *yqiL*) using established amplification methods.[17]

Bioinformatics Analysis

To explore the presence of *desKR* genes across the different strains, all available *S. aureus* genome sequences in the National Center for Biotechnology Information (NCBI) RefSeq database (as of November 30, 2023, totaling 15,626 strains) were downloaded. All sequences were typed using MLST by leveraging the tool available at the MLST website (https://pubmlst.org/organisms/staphylococcus-aureus).[24] Screening for *desK* (Gene ID: 3920139) and *desR* (Gene ID: 3920140) was performed using local BLAST with a minimum identity of 95%. The structural domains of the DesK and DesR proteins were analyzed using the Simple Modular Architecture Research Tool (SMART), and their structures were predicted using SWISS-MODEL.[25,26] Comparative genomic analysis of the *desKR* gene cluster across different strains, including standard strains ST8 (GCA_000013425), ST59 (GCF_000237125), and ST398 (GCF_000009585), was performed and visualized using Clinker.[27]

Construction of Deletion Mutants, Complementation Mutants, and Overexpression Strains

The shuttle plasmids, pKOR1 and pLI50, were acquired from Addgene (plasmids #13573 and #133446). Deletion mutants of *desKR* were constructed using homologous recombination, as described by Bae and Schneewind, with some modifications.[22] Briefly, upstream and downstream DNA fragments of *desKR* were amplified from NCTC8325 chromosomal DNA. These fragments were linked by fusion PCR and cloned into the pKOR1 vector using Gateway BP Clonase II (Thermo Fisher Scientific). The plasmid was then transformed into *Escherichia coli* strains DH5α and DC10B, and electroporated into NCTC8325. Homologous recombination between the plasmid's homology arms and the genome,

Table 1 Strains and Plasmids Used in This Study

Strain or Plasmid	Description	Reference or source
Strains		
ST8 (GCA_000013425)	*S. aureus* for comparative genomic analysis	NCBI
ST59 (GCF_000237125)	*S. aureus* for comparative genomic analysis	NCBI
ST398 (GCF_000009585)	*S. aureus* for comparative genomic analysis	NCBI
DH5α	*E. coli* cloning strain	Invitrogen
DC10B	*E. coli* Δdcm restriction-deficient cloning strain	[18]
NCTC8325	Laboratory strain	[19]
NCTC8325Δ*desKR*	NCTC8325 strain with the *desKR* gene deleted	This study
NCTC8325Δ*desKR*-C	NCTC8325Δ*desKR* strain complemented with the *desKR* gene	This study
ATCC29213	Standard quality-control strain for crystal violet staining assay	[20]
ATCC12228	Standard quality-control strain for crystal violet staining assay	[21]
SA27	Naturally *desKR*-deficient ST398 *S. aureus* strain	This study
SA42	Naturally *desKR*-deficient ST59 *S. aureus* strain	This study
SA27: pLI50	SA27 strain carrying the empty pLI50 vector	This study
SA42: pLI50	SA42 strain carrying the empty pLI50 vector	This study
SA27: pLI50-*desKR*-C	SA27 strain carrying the pLI50-*desKR* vector	This study
SA42: pLI50-*desKR*-C	SA42 strain carrying the pLI50-*desKR* vector	This study
Plasmids		
pKOR1	*S. aureus-E. coli* shuttle vector for constructing deletion mutants	[22]
pLI50	*S. aureus-E. coli* shuttle vector for constructing complementation and overexpression strains	[23]
pLI50-desKR	pLI50 with gene encoding *desKR*	This study

driven by chloramphenicol induction and incubation at 43°C, resulted in deletion of *desKR*. To create complementation mutants, the full-length *desKR* gene and its promoter region were amplified using PCR and ligated into the pLI50 vector. The resulting complementation plasmid, pLI50-*desKR*, was electroporated into the *desKR* deletion mutant. The resultant strain is designated Δ*desKR*-C (*desKR* deletion mutant complemented with the *desKR* gene). The same methodology was applied to construct overexpression *S. aureus* strains SA27 and SA42, resulting in the strains SA27: pLI50-*desKR*-C and SA42: pLI50-*desKR*-C, respectively. The primers used are listed in Table 2.

Minimum Inhibitory Concentrations (MICs) Determination

MICs of oxacillin, ampicillin, gentamicin, linezolid, vancomycin, levofloxacin, moxifloxacin, erythromycin, clindamycin, teicoplanin, tigecycline, and rifampicin were determined using the microdilution broth method. All antimicrobial susceptibility testing and interpretive criteria were performed in accordance with the breakpoints specified in the Clinical and Laboratory Standards Institute guidelines (CLSI, 2023).[28] *S. aureus* ATCC 29213 served as a quality control strain for MIC testing.

Table 2 PCR Primers are Used for PCR Assays

PCR Product	Primer Description	Primer Sequence
gyrB-RT-F	RT-qPCR	ACATTACAGCAGCGTATTAG
gyrB-RT-R	RT-qPCR	CTCATAGTGATAGGAGTCTTCT
icaA-RT-F	RT-qPCR	GTTGGTATCCGACAGTATA
icaA-RT-R	RT-qPCR	CACCTTTCTTACGTTTTAATG
icaD-RT-F	RT-qPCR	TGTTTAGTTGTTCTACTCGTTTA
icaD-RT-R	RT-qPCR	CTCTTCCTCTCTGCCATT
icaB-RT-F	RT-qPCR	CCTATCCTTATGGCTTGATGA
icaB-RT-R	RT-qPCR	CATTGGAGTTCGGAGTGA
icaC-RT-F	RT-qPCR	AATGGAGACTATTGGAACC
icaC-RT-R	RT-qPCR	AAAGAATGAGAAAGCA AATC
atl-RT-F	RT-qPCR	GGCTTAGGTGT GGTG
atl-RT-R	RT-qPCR	TATGGCTC AATGGTAA
lytM-RT-F	RT-qPCR	CATTCGTAGATGC AAG
lytM-RT-R	RT-qPCR	TGTGTAGTCATTGT
sle1-RT-F	RT-qPCR	ACCAGTATT GTCACCAA
sle1-RT-R	RT-qPCR	CCA TATTAG TTCCACCAAT
desKR-U-F	Gene knockout	GGGGACAA TTTG AAAAAAGCAGGCTAATCATAATGGCACTATCAA
desKR-U-R	Gene knockout	TTTG AGATCCAGCCATAGACGATATTTCAGCAAT
desKR-D-F	Gene knockout	TTGCT AATATCGTCTATGGCTGGATCTAAATACAAA
desKR-D-R	Gene knockout	GC GACCA TTGTACAAGAAAGCTGGGTACGCACTATGGTTATTATG
desKR-C-F	Complementation	CGCGGATCCGCAATAGCGATATTAGTTAT
desKR-C-F	Complementation	CCCAAGCTTGTATTTAGATCCAGCCTTT

Mouse Bloodstream Infection Model

Age-matched (6-week-old female wild-type (WT) BALB/c mice were purchased from Yangzhou University with a permit and used in this study. Mice were randomly divided into four groups (n=10 per group). *S. aureus* strains NCTC8325, Δ*desKR*, and Δ*desKR*-C were cultured in TSB until the post-exponential phase. Bacterial cells were collected by centrifugation, washed thrice with sterile PBS, and resuspended in PBS. Subsequently, 100 μL of PBS containing 1×10^{7} colony-forming units (CFU) was injected into the tail vein, with sterile PBS serving as a control to exclude the effects of the solvent and the operation. Following inoculation, the health status of the mice was continuously monitored and survival rates were recorded over a 7-day period.

Skin Abscess Model

Forty 6-week-old female BALB/c mice were randomly divided into four groups, with ten mice in each group. After preparing the bacterial suspensions as described above, 100 μL of 1×10^{7} CFU was injected subcutaneously into the flank of each mouse. Control mice received 100 μL of sterile PBS. Abscess size was measured 48 h later using the formula $A = \pi \times (L \times W)$,

where L and W are the length and width, respectively. Following euthanasia, the skin tissues were dissected and homogenized, and the bacterial load was quantified by serial dilution on blood agar plates.

Nasal Colonization Model

The nasal tissue colonization experiment was conducted with modifications to previously described methods.[29] Forty 6-week-old female BALB/c mice were randomly divided into four groups, with ten mice in each group. Each received a 30 µL droplet containing 1×10^7 CFU of NCTC8325, Δ*desKR*, or Δ*desKR*-C in their nostrils. Control mice received 30 µL of sterile PBS. After 48 h, the mice were euthanized, nasal tissues were collected and decontaminated with 70% ethanol, homogenized, diluted, and plated on blood agar for overnight incubation to count CFU.

Growth Curves Assay and Viable Cell Count

Log-phase *S. aureus* strains NCTC8325, Δ*desKR*, and Δ*desKR*-C were inoculated into TSB and incubated at 37°C with shaking at 220 rpm. Sterile TSB served as a control. Bacterial growth was monitored by measuring the optical density at 600 nm over a 24-hour period. After 24 h of growth, bacterial suspensions were serially diluted and plated on blood agar plates. Following overnight incubation, CFU were counted to determine viable cell counts. All experiments were performed in triplicate.

Crystal Violet Staining Assay

S. aureus strains NCTC8325, Δ*desKR*, and Δ*desKR*-C were cultured overnight in TSB at 37°C with shaking (220 rpm). The cultures were diluted 1:200 in TSBG (containing 0.5% glucose) and were added to sterile 96-well plates. After incubation at 37°C for 24 h, the supernatant was discarded and the biofilms were gently washed three times with sterile PBS. The plates were air-dried and the biofilms were fixed with anhydrous methanol for 10 min. The liquid was discarded and the biofilms were stained with crystal violet (C0121, Biyuntian, China) for 20 min. The plates were gently washed with running water and air dried at room temperature. The optical density was measured at 600 nm. *S. aureus* ATCC 29213 served as a positive control, whereas sterile TSBG and *S. epidermidis* ATCC 12228 served as negative controls. The experiments were repeated three times.

Confocal Laser Scanning Microscope (CLSM) Analysis

S. aureus biofilms were prepared in 20 mm glass-bottom cell culture dishes (FCFC020, Biyuntian, China) under culture conditions similar to those described above. The biofilms were washed three times with sterile PBS and stained with 500 µL of fluorescent dye containing 0.02% SYTO 9 (Thermo Scientific, United States) and 0.067% propidium iodide (ST512, Biyuntian, China). The dishes were incubated in the dark for 30 min. The biofilm structure was observed using a CLSM system (Nikon, Tokyo, Japan).

Quantification of Polysaccharide Intercellular Adhesin (PIA)

PIA was quantified with minor modifications as previously described.[30,31] Briefly, overnight cultures of *S. aureus* strains NCTC8325, Δ*desKR*, and Δ*desKR*-C were diluted 1:100 in TSBG and incubated in 6-well plates at 37°C for 24 h. After washing with PBS, biofilms were scraped, resuspended in 500 µL EDTA (0.5 M, pH 8.0), and boiled. Supernatants were digested with proteinase K, spotted onto methanol-activated PVDF membranes, blocked, and probed with WGA-HRP. Detection was done using ECL, and grayscale values were analyzed with ImageJ.

Extracellular DNA (eDNA) Quantification Assay

Isolation and quantification of eDNA were performed as previously described.[32] *S. aureus* strains NCTC8325, Δ*desKR*, and Δ*desKR*-C were cultured in six-well plates as described above. After biofilm formation and subsequent processing, the biofilms were resuspended in 500 µL of EDTA (0.5 M) and placed on ice for 1 h. Next, the biofilms were resuspended in buffer (50 mM Tris-HCl, pH 8.0; 10 mM EDTA, 500 mM NaCl). The samples were centrifuged at 16,000 rpm for 10 min and the supernatant was transferred to new tubes. Equal volumes of phenol-chloroform-isoamyl alcohol (25:24:1) and chloroform-isoamyl alcohol (24:1) were added. After thorough mixing, the samples were stored at −20°C overnight, and 10% 3M sodium

acetate ethanol was added. Subsequently, the eDNA was collected by centrifugation at 16,000 rpm for 10 min, washed with 75% ethanol, and dissolved in TE buffer. The eDNA was quantified using a NanoDrop 2000 spectrophotometer. Relative eDNA secretion was determined by dividing the total eDNA (ng) by the biofilm OD_{600} value.

Autolysis Assay

To determine the effect of *desKR* deletion on *S. aureus* autolysis, an autolysis assay was performed as previously described.[33] Briefly, log-phase cultures of *S. aureus* NCTC8325, Δ*desKR*, and Δ*desKR*-C were centrifuged, washed twice with sterile distilled water, resuspended in 50 mM Tris-HCl buffer (pH 7.5) containing 0.05% (v/v) Triton X-100, and adjusted to an OD_{600} of 1.0. The suspensions were incubated at 37°C with shaking at 220 rpm. The OD_{600} was measured every 1 h for 5 h to monitor the autolysis.

Reverse Transcription Quantitative PCR (RT-qPCR)

S. aureus strains NCTC8325, Δ*desKR*, and Δ*desKR*-C were cultured in TSBG at 37°C with shaking (220 rpm) for 4 h. Total RNA was isolated using a Total RNA Purification Kit (Sangon Biotech, China), according to the manufacturer's protocol. Total RNA was reverse-transcribed into cDNA using a PrimeScript RT Reagent Kit with gDNA Eraser (Takara Bio, Inc). Gene expression was normalized to the level of *gyrB* and calculated using the $2^{-\Delta\Delta CT}$ method. RT-qPCR was performed using the ChamQ Universal SYBR qPCR Master Mix (Vazyme) on a Roche LightCycler 480 II System (Roche). The primer pairs are shown in Table 2. Each reaction was performed in triplicate.

Statistical Analysis

All experimental data were analyzed by unpaired Student's *t*-test or one-way ANOVA (analysis of variance) using Prism 8.0 software (GraphPad Inc., San Diego, CA, USA). $P < .05$ was statistically considered to be significant. Error bars in the figures represent the standard deviation of the dataset (mean ± standard deviation). $^{*}P < .05$, $^{**}P < .01$, $^{***}P < .001$, $^{****}P < .0001$.

Results

Distribution of desKR in S. Aureus

We retrieved 15,626 *S. aureus* whole genome assemblies from the NCBI RefSeq database (on November 30, 2023). Local BLAST analysis revealed that *desK* and *desR* were present in 84.85% (13,259/15,626) and 85.34% (13,336/15,626) of the strains, respectively. MLST typing of 15,626 *S. aureus* strains showed that the carriage rates of *desK* and *desR* varied among different sequence types (STs). The detailed distributions of *desKR* in different STs are listed in Table 3. Notably, *desK* was detected in only a small fraction of ST398 (2/1180, 0.17%) and ST59 (1/229, 0.44%) strains, while *desR* was similarly detected at low frequencies in ST398 (3/1180, 0.25%) and ST59 (1/229, 0.44%) strains. However, the prevalence of *desKR* in other STs (except for ST36) ranged from 89.46% to 100% for *desK* and from 97.92% to 100% for *desR*. The heatmap (Figure 1A) provides a more intuitive representation of the lineage-dependent prevalence of *desKR*. The locus tags for *desK* and *desR* in NCTC 8325 were *SAOUHSC_01313* and *SAOUHSC_01314*, respectively, with *desK* located upstream of *desR* (Figure 1B).

Structural Domain Analysis of DesKR in S. Aureus

The *desKR* two-component system in *S. aureus* is composed of a histidine kinase, DesK, and a response regulator, DesR. DesK is a protein consisting of 363 amino acids, while DesR is composed of 200 amino acids. To understand the potential functions of these proteins, we performed a detailed structural domain analysis using the SMART database.

DesK was predicted to be a membrane-anchored protein characterized by five transmembrane (TM) domains, which are crucial for spanning the cell membrane (Figure 2A and B). These TM domains suggest that DesK likely plays a role in sensing environmental or membrane-associated signals. Structural analysis further revealed that DesK contains a HisKA_3 domain (spanning residues 176–242), responsible for dimerization and containing a critical phosphoacceptor histidine residue (Figure 2A and B). The presence of this domain is indicative of its role in signal transduction via

Table 3 The Presence of desKR in Different STs

	desK Positive Strains		*desR* Positive Strains	
MLST	**No./total**	**Percentage (%)**	**No./total**	**Percentage (%)**
ST5	2862/2946	97.15%	2903/2946	98.54%
ST8	2401/2449	98.04%	2435/2449	99.43%
ST22	1464/1486	98.52%	1474/1486	99.19%
ST398	2/1180	0.17%	3/1180	0.25%
ST105	629/634	99.21%	631/634	99.53%
ST239	314/351	89.46%	349/351	99.43%
ST45	341/349	97.71%	349/349	100.00%
ST1	319/337	94.66%	330/337	97.92%
ST30	327/337	97.03%	336/337	9[illegible]70%
ST9	285/294	96.94%	292/294	99.[illegible]
ST59	1/229	0.44%	1/229	0.44%
ST15	206/213	96.71%	210/213	[illegible]8.59%
ST36	201/201	100.00%	0/201	0.00%
ST121	197/197	100.00%	197/197	100.00%
ST7	185/185	100.00%	185/185	100.00%
ST97	165/172	95.9[illegible]	169/172	98.26%
ST188	145/148	97.97%	147/148	99.32%
ST6	122/1[illegible]	[illegible]7.60%	125/125	100.00%
ST72	[illegible]23/1[illegible]	[illegible]	124/125	99.20%
ST88	97/98	98.98%	98/98	100.00%
Others	[illegible]73/3570	80.48%	2978/3570	83.42%
Total	13259/[illegible]626	84.85%	13,336/15,626	85.34%

autophosphorylation. Additionally, DesK features a HATPase_c domain (residues 275–361), which is characteristic of histidine kinases' ATPases and essential for catalyzing the phosphorylation of the histidine residue within the HisKA_3 domain. This phosphorylation event is a critical step in transferring the phosphate group to the response regulator DesR.

DesR, the response regulator, is composed of two main domains: an REC (Receiver) domain (residues 2–115) and a LuxR-type Helix-Turn-Helix (HTH) domain (residues 137–194) (Figure 2C and D). The REC domain functions as the phosphoacceptor site, where it receives the phosphate group from the histidine residue in DesK. This phosphorylation typically induces a conformational change in DesR, which is crucial for its regulatory function. The conformational change activates the LuxR-type HTH domain, enabling DesR to bind to specific DNA sequences in the promoters of downstream genes. This binding is essential for the regulation of gene expression, either activating or repressing target genes involved in biofilm formation and other cellular processes.

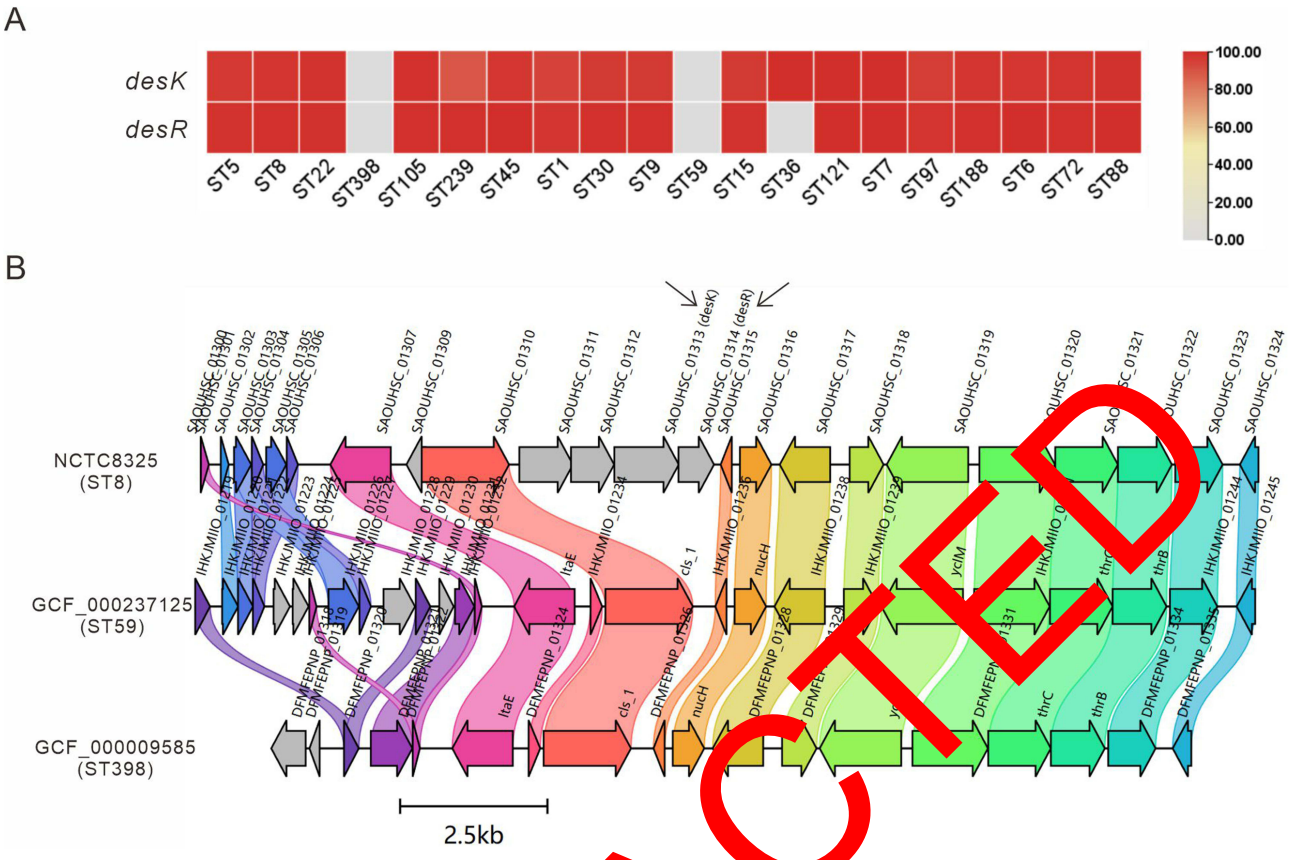

Figure 1 Prevalence and genomic context of the two-component regulatory system *desKR*. (**A**) Heatmap showing the prevalence of *desKR* in different sequence types (STs). (**B**) Genomic context of *desKR*. The reference strain NCTC 8325 (ST8), containing the *desKR* genes was selected, and strains GCF_000237125 (ST59) and GCF_000009585 (ST398) from NCBI were included for comparison. Black arrows indicate the positions of *desK* and *desR* in NCTC 8325.

The Impact of desKR Deletion on S. aureus Antibiotic Susceptibility

To further investigate the biological function of *desKR*, we constructed a *desKR* deletion mutant (Δ*desKR*) and its complemented strain (Δ*desKR*-C). MICs of the antimicrobial agents were determined using the broth microdilution method. As shown in Table 4, the deletion of *desKR* resulted in a 2- to 4-fold increase in the MICs of oxacillin, ampicillin, vancomycin, and teicoplanin. However, the MICs of gentamicin, linezolid, levofloxacin, moxifloxacin, erythromycin, tigecycline, rifampicin, and clindamycin were not affected. These results indicate that *desKR* specifically modulates resistance to β-lactams and glycopeptides.

The Impact of desKR on S. aureus Acute Pathogenicity, Adhesion, Colonization, and Growth

To investigate the influence of *desKR* on the in vivo pathogenicity of *S. aureus*, we established a bloodstream infection model. Thirty-six hours post-infection, the mortality rates of the mice in the NCTC8325, Δ*desKR*, and Δ*desKR*-C groups were consistently 70%, with no statistically significant differences (Figure 3A). To assess the effect of *desKR* on the ability of *S. aureus* to form skin abscesses, we established a mouse skin abscess model. As shown in Figure 3B, there were no significant differences in the area of skin abscesses between the wild-type NCTC8325, Δ*desKR*, and Δ*desKR*-C groups. Moreover, colony counting of the abscess tissues demonstrated no significant differences in the bacterial load among the three groups (Figure 3C). Collectively, these findings suggest that the *desKR* two-component system does not significantly affect acute pathogenicity of *S. aureus*.

Given that *S. aureus* nasal carriage is a well-established risk factor for subsequent infections, we also established a mouse nasal colonization model to investigate the effect of *desKR* on the adhesion and colonization ability of *S. aureus*.

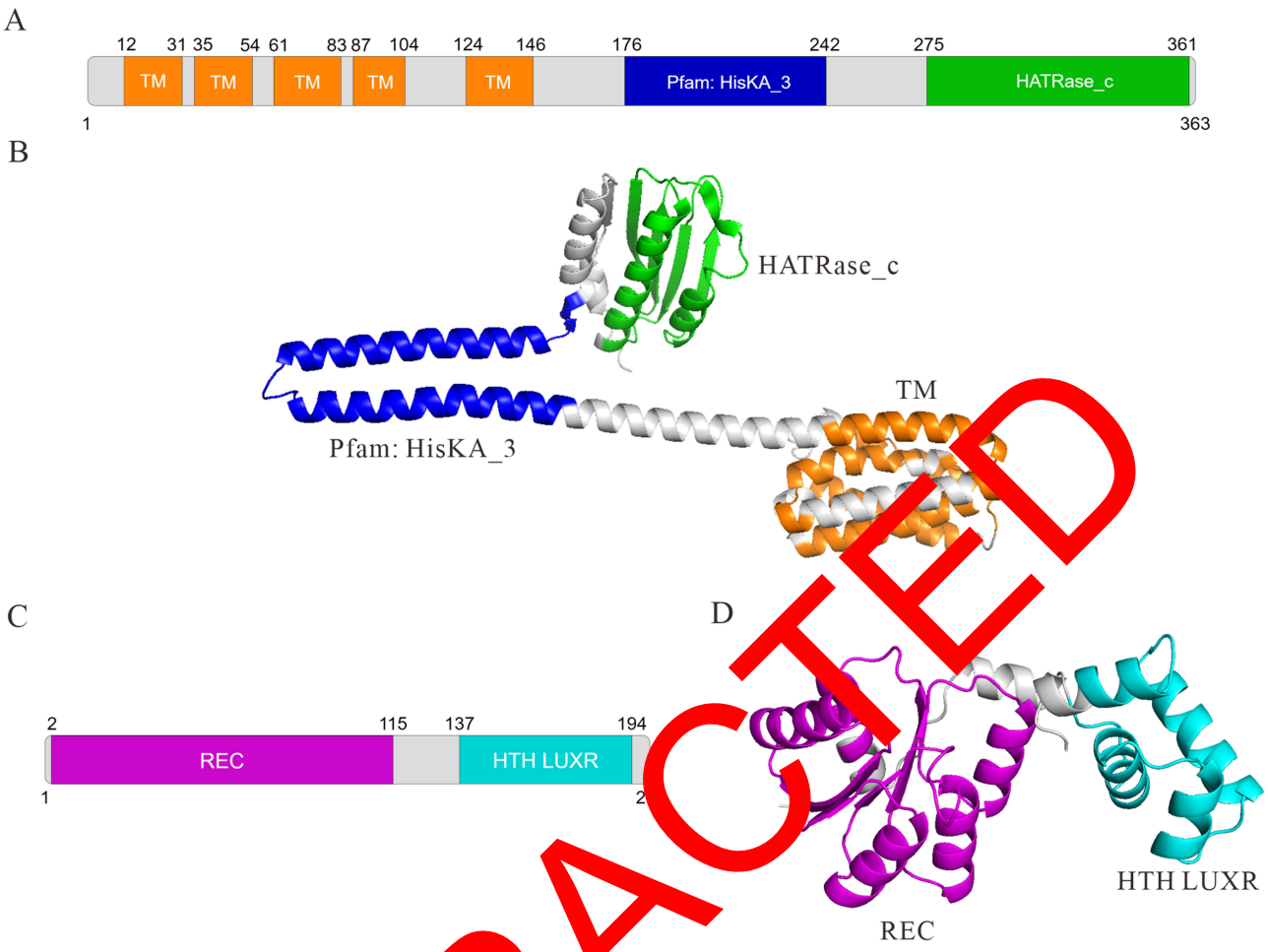

Figure 2 Simple Modular Architecture Research Tool (SMART) and SWISS-MODEL Analysis of DesKR. (**A**) Predicted domain of DesK based on SMART (http://smart.embl-heidelberg.de/). (**B**) 3D protein simulation of DesK using the SWISS-MODEL web server. (**C**) Predicted domain of DesR based on SMART. (**D**) 3D protein simulation of DesR using the SWISS-MODEL web server.

Forty-eight hours after intranasal inoculation with 30 μL of a suspension containing 1.5×10^7 CFU of *S. aureus*, the CFU count in the nasal tissue revealed a significantly lower bacterial burden in mice infected with Δ*desKR* compared to the NCTC8325 control group (1.68×10^3 CFU/mL vs 2.78×10^3 CFU/mL, $P < 0.0001$) (Figure 3D). In contrast, the bacterial burden in the mice infected with Δ*desKR*-C was comparable to that in the control group. These results indicate that *desKR* plays a role in modulating the adhesion and colonization ability of *S. aureus*.

Table 4 MIC Determination of Antibiotics for NCTC8325 and ΔdesKR

Antibiotics	NCTC8325	Δ*desKR*
Oxacillin	0.125	0.25
Ampicillin	0.125	0.5
Gentamicin	0.5	0.5
Linezolid	4	4
Vancomycin	0.5	2

(*Continued*)

Table 4 (Continued).

Antibiotics	NCTC8325	Δ*desKR*
Levofloxacin	0.125	0.125
Moxifloxacin	0.25	0.25
Erythromycin	0.5	0.5
Clindamycin	0.125	0.125
Teicoplanin	1	2
Tigecycline	0.125	0.125
Rifampicin	0.125	0.125

To rule out the possibility that the *desKR* two-component regulatory system reduced the adhesion ability of *S. aureus* by affecting its normal growth, we evaluated the growth curves at 37°C. As shown in Figure 3E, no significant differences were observed in the growth trends of NCTC8325, Δ*desKR*, or Δ*desKR*-C. Furthermore, the viable bacterial count results showed that the cell densities of *S. aureus* strains NCTC8325, Δ*desKR*, and Δ*desKR*-C remained consistent in the plateau growth phase (24 h), as illustrated in Figure 3F. These data provide evidence that the observed reduction in

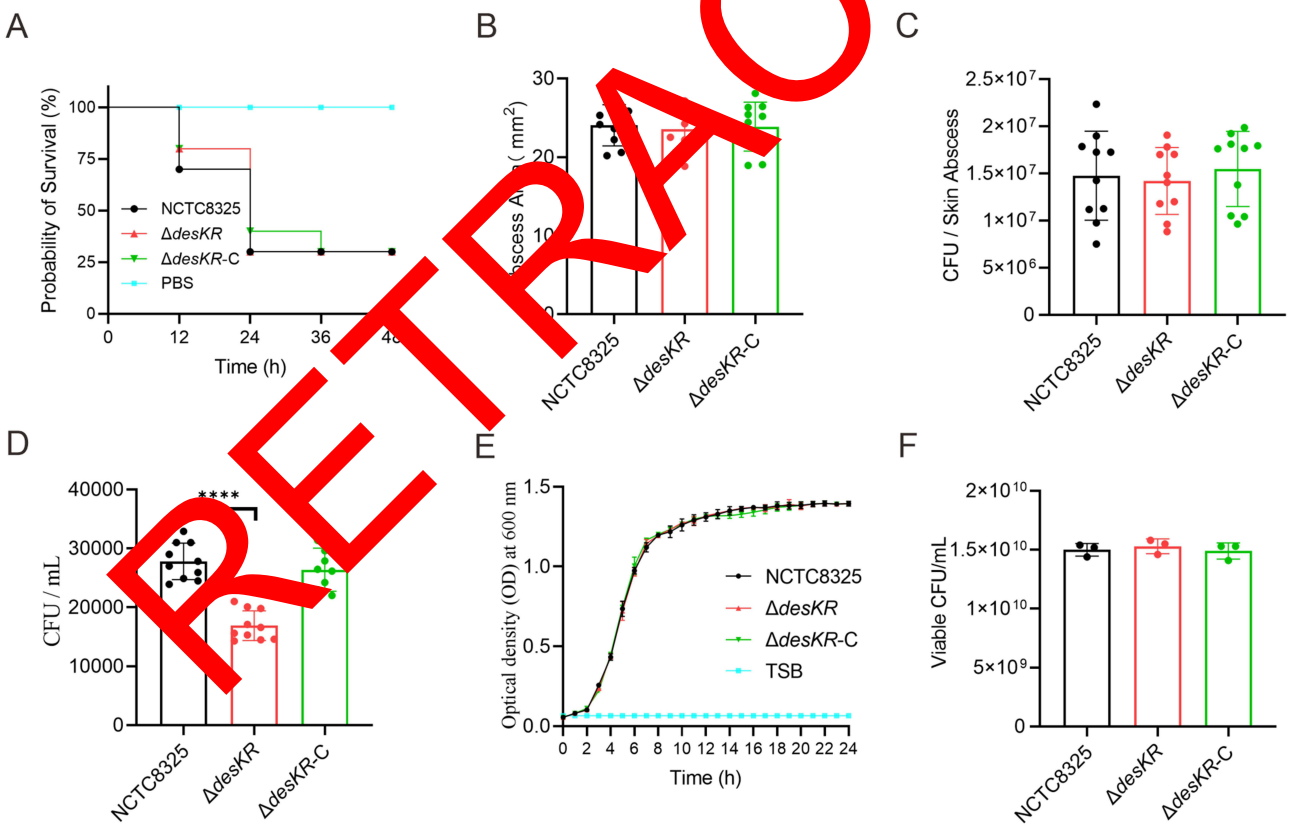

Figure 3 Impacts of *desKR* deletion on *S. aureus* virulence, adhesion, colonization, and growth. (**A**) Mouse bloodstream infection model. Kaplan-Meier estimates of survival in mice infected with *S. aureus* NCTC8325, Δ*desKR*, and Δ*desKR*-C. Sterile PBS was used as a control to exclude the influence of solvents and manipulation. (**B**) Mouse skin abscess model. Skin abscess area in mice (n=10 per group) two days after infection with *S. aureus* NCTC8325, Δ*desKR*, and Δ*desKR*-C. (**C**) Bacterial burden in mouse abscess homogenates determined by serial dilution and culturing on blood agar plates. (**D**) Mouse nasal colonization model. Bacterial burden in nasal tissues of mice (n=10 per group) 48 hours after infection with *S. aureus* NCTC8325, Δ*desKR*, and Δ*desKR*-C. (**E**) 24-hour growth curves of *S. aureus* NCTC8325, Δ*desKR*, and Δ*desKR*-C. (**F**) Colony-forming units of *S. aureus* NCTC8325, Δ*desKR*, and Δ*desKR*-C cultures following 24 hours of incubation. ****P < 0.0001.

nasal colonization by the Δ*desKR* strain is not attributable to impaired growth but rather to a specific effect on adhesion and colonization.

ΔdesKR Exhibits Significantly Weakened Biofilm Formation Ability

Adhesion to biological and non-biological surfaces is the first step in the formation of *S. aureus* biofilms. To investigate the effect of *desKR* on biofilm formation by *S. aureus*, we conducted a semi-quantitative crystal violet assay. As depicted in Figure 4A, crystal violet staining revealed that both NCTC8325 and Δ*desKR*-C formed distinct adhesions with OD_{600} values of 2.91 ± 0.04 and 2.88 ± 0.10, respectively. In contrast, the adhesion formed by Δ*desKR* was considerably

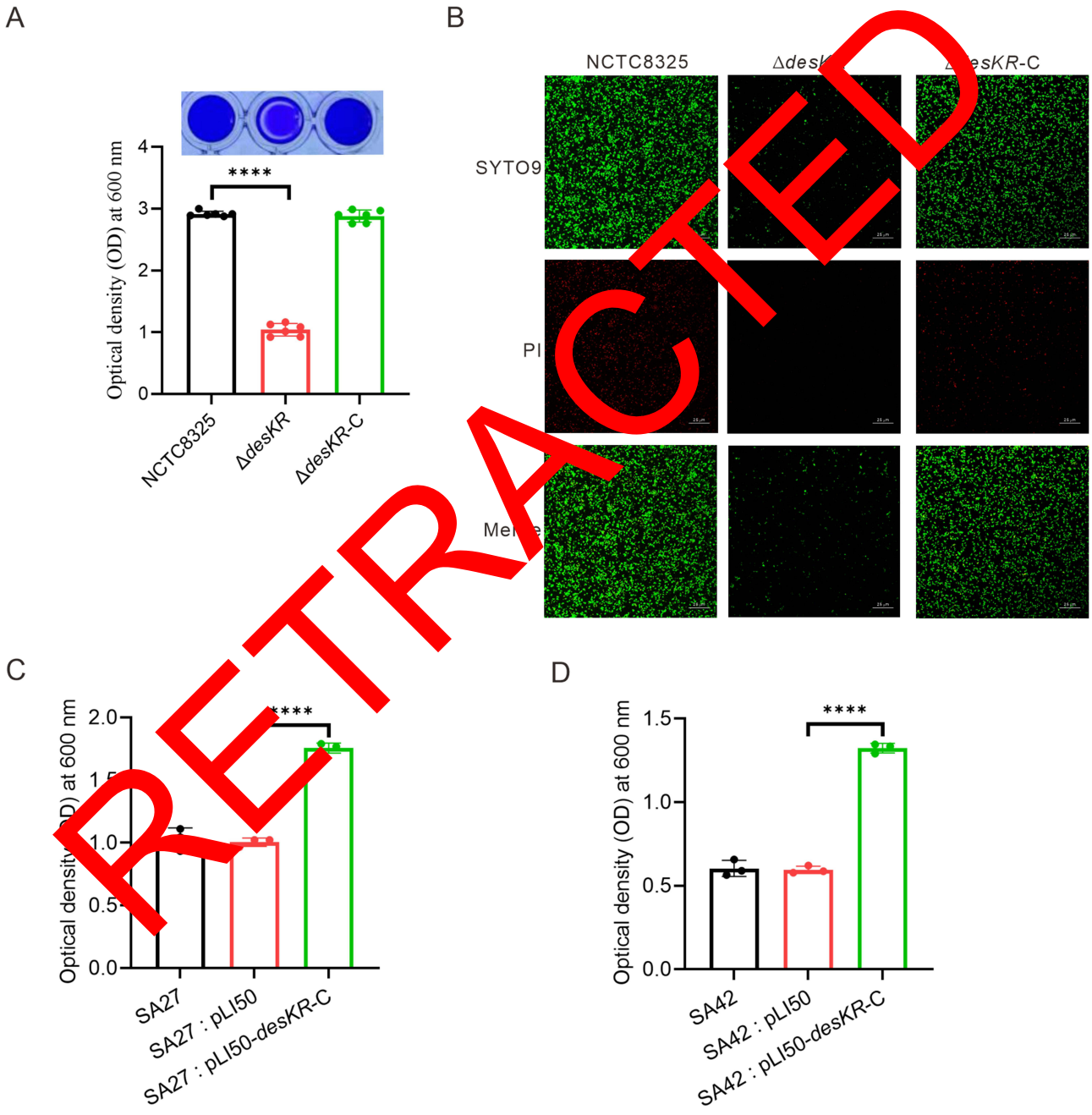

Figure 4 Impacts of *desKR* on *S. aureus* biofilm formation ability. (**A**) Detection of biofilm formation ability of NCTC8325, Δ*desKR*, and Δ*desKR*-C using crystal violet staining assay. (**B**) Confocal laser scanning microscopy images of biofilms formed by NCTC8325, Δ*desKR*, and Δ*desKR*-C. (**C**) Impacts of *desKR* overexpression on the biofilm formation ability of clinical strain SA27 (ST59). (**D**) Impacts of *desKR* overexpression on the biofilm formation ability of clinical strain SA42 (ST398). ****P < 0.0001.

weaker, with an OD_{600} value of 1.04 ± 0.10. Notably, the amount of biofilm formed by Δ*desKR* was reduced by 64.4% compared to NCTC8325 ($P < 0.0001$), highlighting the significant impact of *desKR* on biofilm formation.

To further elucidate the changes in biofilm formation at higher resolutions, CLSM analysis was employed. To differentiate between live and dead cells within the biofilm, we utilized a fluorescent dye staining technique, wherein SYTO9 dye was used to stain live bacteria green, whereas propidium iodide dye penetrated the membranes of dead cells, causing them to appear red. As illustrated in Figure 4B, the biofilms formed by NCTC8325 and Δ*desKR*-C on glass dishes comprised a large number of live and dead cells, forming dense biofilm structures. In stark contrast, the biofilm structure of Δ*desKR* was sparse, with few accumulations of cell clusters and only a small number of live and dead cells attached to the culture surface. These findings strongly suggest that *desKR* plays a crucial role in promoting the formation of *S. aureus* biofilms, and that its deletion significantly impairs biofilm development.

Overexpression of desKR Enhances Biofilm Formation Ability in ST398 and ST59 Strains

To investigate whether promotion of *S. aureus* biofilm formation by *desKR* is a lineage-specific mechanism, we expressed *desKR* in strains lacking the *desKR* gene. We selected one ST398 strain (SA27) and one ST59 strain (SA42) of *S. aureus*. Both strains were isolated from bovine subclinical mastitis. Polymerase chain reaction (PCR) confirmed that SA27 and SA42 did not carry the *desKR* gene. We electroporated the empty vector pLI50 and the complementation plasmid pLI50-*desKR*-C into the SA27 and SA42 strains and then performed a crystal violet staining experiment to detect changes in their biofilm formation ability. As shown in Figure 4C and D, overexpression of *desKR* in the ST398 and ST59 strains significantly enhanced their biofilm formation ability. Specifically, the biofilm formation ability of SA27: pLI50-*desKR*-C (1.76 ± 0.04) was significantly higher than that of the control group SA27: pLI50 (1.005 ± 0.03) ($P < 0.0001$). Similarly, the biofilm forming ability of SA42: pLI50-*desKR*-C (1.32 ± 0.03) was significantly higher than that of the control group SA42: pLI50 (0.60 ± 0.02) ($P < 0.0001$). These results demonstrate that the introduction of *desKR* into strains naturally lacking this two-component system can enhance biofilm formation regardless of the specific lineage.

desKR Affects the Synthesis of PIA and the Release of eDNA

PIA and eDNA are important components of *S. aureus* biofilm matrix. To investigate the mechanism by which *desKR* affects biofilm formation, we used an immunoblot assay to quantify PIA production in biofilms. As shown in Figure 5A, compared to the wild-type strain NCTC8325, the PIA production of Δ*desKR* was significantly reduced, while the PIA production of Δ*desKR*-C was significantly restored. To determine whether *desKR* affects eDNA release, we extracted eDNA and performed qualitative detection. As shown in Figure 5B, the amount of eDNA released by the Δ*desKR* strain was slightly lower than that of the wild-type strain (33.04 ± 2.17 vs 38.76 ± 3.12, $P = 0.0042$), while the eDNA release of Δ*desKR*-C was somewhat restored.

Cell lysis is a critical pathway for the release of eDNA, which plays a key role in biofilm development. The autolysis assay offers valuable insights into whether *desKR* modulates cell wall integrity or autolytic activity, both of which are crucial for biofilm formation and stability. To further assess the effect of *desKR* on eDNA release in *S. aureus*, we used Triton X-100 to induce autolysis. As shown in Figure 5C, the autolysis rate of Δ*desKR* between 2–4 h was slightly lower than that of NCTC8325 and Δ*desKR*-C.

desKR May Primarily Affect the Biofilm Formation Ability of S. aureus by Influencing the Expression of the ica Operon

To investigate the mechanism by which *desKR* regulates biofilm formation in *S. aureus*, we used RT-qPCR to analyze differences in gene transcription. As shown in Figure 6, in Δ*desKR*, the four genes of the ica operon (*icaA, icaD, icaB, icaC*) that encode PIA biosynthesis were downregulated to 17.03%-19.44% of the NCTC8325 levels ($P < 0.0001$). In contrast, *icaR*, which can directly negatively regulate the expression of the *ica* operon, was significantly upregulated to 5.48 times that of NCTC8325 ($P < 0.0001$). The expression of these genes in the Δ*desKR*-C strain was restored to levels

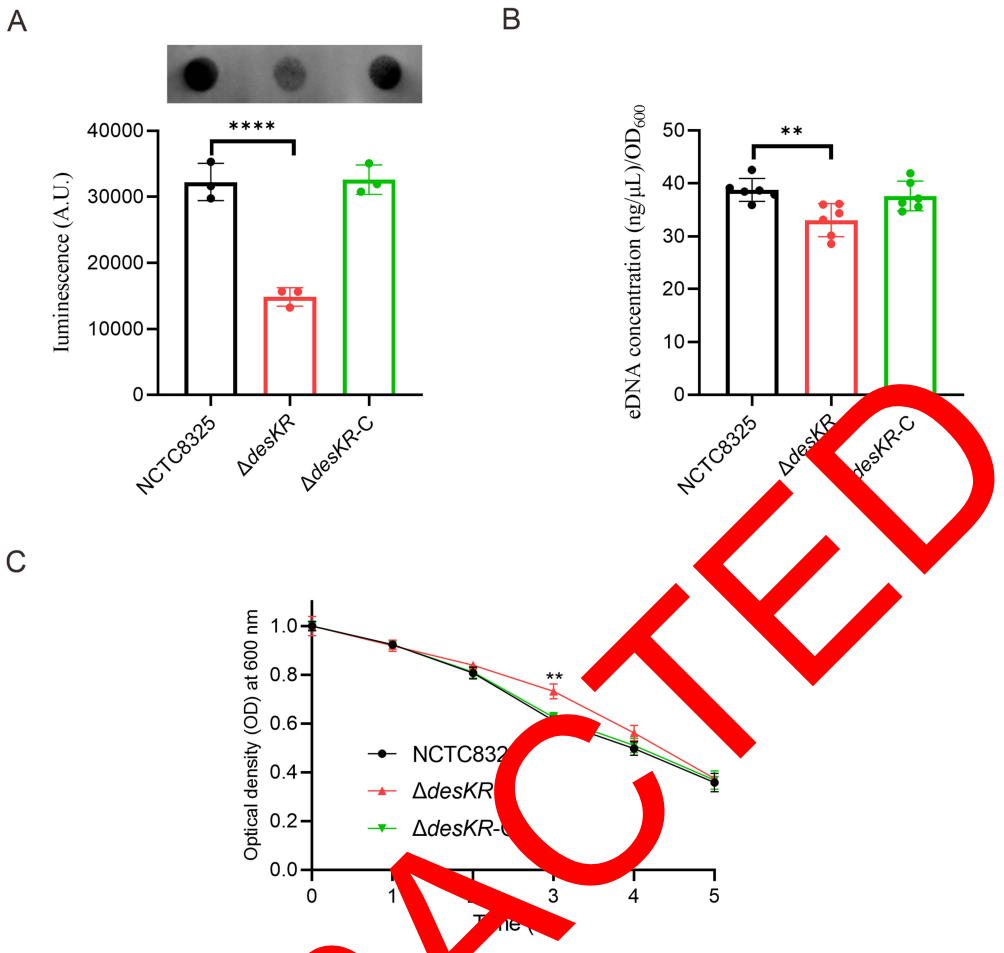

Figure 5 Impacts of *desKR* deletion on *S. aureus* biofilm matrix components. (**A**) PIA production of *S. aureus* NCTC8325, Δ*desKR*, and Δ*desKR*-C. (**B**) Quantification of eDNA in *S. aureus* NCTC8325, Δ*desKR*, and Δ*desKR*-C. (**C**) Autolysability of *S. aureus* NCTC8325, Δ*desKR*, and Δ*desKR*-C. **P < 0.01; ****P < 0.0001.

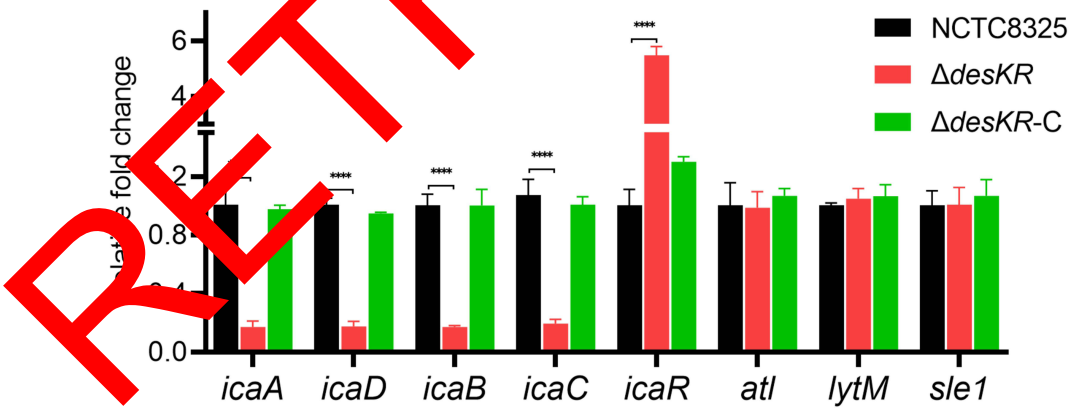

Figure 6 RT-qPCR detection of the impacts of *desKR* deletion on the expression of biofilm-related genes. The relative expression level of the wild-type strain NCTC8325 was set to 1. ****P < 0.0001.

similar to those in the wild-type strain. Furthermore, we detected the expression levels of autolysis-related genes, including *atl* encoding autolysin, *lytM* encoding endopeptidase, and *sle1* encoding l-lysine aminopeptidase. The results showed that, compared with NCTC8325, the expression levels of *atl, lytM*, and *sle1* in Δ*desKR* and Δ*desKR*-C were not

significantly changed. Therefore, we concluded that *desKR* primarily changes the biofilm formation ability of *S. aureus* by affecting the expression of the *ica* operon.

Discussion

The emergence and rapid spread of antibiotic-resistant *S. aureus* pose significant threats to public health worldwide.[35] The ability of *S. aureus* to form biofilms further exacerbates this problem, as biofilm-associated infections are notoriously difficult to treat due to their increased tolerance to antibiotics and host immune responses.[2] Therefore, a deeper understanding of the molecular mechanisms governing biofilm formation in *S. aureus* is crucial for developing effective strategies to combat biofilm-related infections. In this study, we investigated the distribution and biological functions of the *desKR* two-component system in *S. aureus*. Our bioinformatic analysis revealed that the prevalence of *desKR* varies among different *S. aureus* lineages, with notably low carriage rates in the ST398 and ST59 strains. This finding suggests that the acquisition and maintenance of *desKR* may be influenced by lineage-specific evolutionary pressures.

Protein structural analysis revealed that DesKR possesses the typical structural features of a two-component regulatory system, including the transmembrane domain of HK, His dimerization phosphate acceptor domain, ATPase domain, and the receiver and effector domains of RR. These structural domains form the basis for signal transduction in the two-component regulatory system.[5] The presence of transmembrane domains in DesK suggests its role in signal sensing, while the HisKA-3 and HATPase_c domains highlight its function as a histidine kinase. The REC and LuxR-type HTH domains in DesR indicate their role as transcriptional regulators that modulate the expression of genes in response to the signal sensed by DesK.[36]

Two-component systems (TCSs) in bacteria, including *S. aureus*, are critical for sensing environmental stress and regulating gene expression to adapt to various conditions.[37] The VraSR TCS, for instance, is well-documented for its essential role in the cell wall stress response and antibiotic resistance in *S. aureus*.[38,39] Building on this, it is reasonable to hypothesize that the *desKR* TCS may function similarly, particularly in modulating genes involved in peptidoglycan biosynthesis or turnover—processes that are directly targeted by β-lactams and glycopeptides. To test this hypothesis, we constructed a *desKR* deletion mutant and performed antibiotic susceptibility assays, which revealed that *desKR* significantly influences the resistance of *S. aureus* to β-lactams and glycopeptides. Notably, the MIC for antibiotics that do not target cell wall synthesis (eg, gentamicin, linezolid, fluoroquinolones) remained unchanged. This suggests that *desKR* does not broadly affect antibiotic resistance but instead exerts a specific regulatory effect on cell wall-targeting antibiotics. These results support the hypothesis that *desKR* modulates pathways directly involved in cell wall synthesis or modification, which are the primary targets of β-lactam and glycopeptide antibiotics. This finding is consistent with previous reports implicating two-component systems in the regulation of antibiotic resistance in *S. aureus*.[40] However, the precise molecular mechanisms by which *desKR* influences antibiotic resistance remain to be elucidated. Future studies should focus on identifying the downstream targets of *desKR* and unravel the regulatory networks that link this two-component system to antibiotic resistance. Interestingly, although *desKR* did not significantly affect the acute pathogenicity of *S. aureus* in our bloodstream infection and skin abscess models, it played a crucial role in modulating the adhesion and colonization ability of *S. aureus*. This finding is particularly relevant, as *S. aureus* nasal carriage is a well-established risk factor for subsequent infections.[41] Our results suggest that *desKR* may contribute to the persistence of *S. aureus* in the host, potentially increasing the risk of infection. This highlights the potential of *desKR* as a novel strategy to prevent *S. aureus* colonization and subsequent infections.

One of the most striking findings of our study was the significant effect of *desKR* on the biofilm forming ability of *S. aureus*. The deletion of *desKR* resulted in a 64.4% reduction in biofilm formation, whereas overexpression of *desKR* in the ST398 and ST59 strains, which naturally lacking this two-component system enhanced their biofilm formation ability. These results demonstrate that *desKR* is a key regulator of biofilm formation in *S. aureus*, and its presence or absence can significantly influence the biofilm forming capacity of *S. aureus*, regardless of the specific lineage. The ability of *desKR* to enhance biofilm formation in diverse genetic backgrounds highlights its potential as a target for anti-biofilm strategies and underscores the importance of further investigating the molecular mechanisms by which it regulates this critical aspect of *S. aureus* pathogenesis.

Our study further revealed that *desKR* affects the synthesis of PIA and the release of eDNA, two essential components of the *S. aureus* biofilm matrix.[42] These results suggest that *desKR* may promote the synthesis of PIA and release of eDNA in *S. aureus*. The reduction in PIA production in the Δ*desKR* strain is consistent with the observed impairment in biofilm formation, as PIA is a key component of the biofilm matrix that facilitates cell-cell adhesion and structural integrity. The significant downregulation of *ica* operon genes in the Δ*desKR* strain is consistent with the observed reduction in PIA production and impaired biofilm formation. The *ica* operon is responsible for the synthesis of PIA polysaccharide, which is a crucial component of the biofilm matrix. The concomitant upregulation of *icaR*, a negative regulator of the *ica* operon, suggests that *desKR* may influence PIA synthesis by modulating *icaR* expression. Furthermore, although we observed a slower autolysis rate in the Δ*desKR* strain, the lack of significant changes in the expression of autolysis-related genes (*atl, lytM*, and *sle1*) indicates that *desKR* does not influence autolysin production at the transcriptional level but may affect post-translational processing of autolysins. This finding, coupled with the modest changes in eDNA release observed in the Δ*desKR* strain, suggests that the biofilm-promoting effect of *desKR* is largely dependent on its influence on PIA synthesis via the *ica* operon. These findings provide valuable insights into the molecular basis of *desKR*-mediated regulation of biofilm formation in *S. aureus*.

DesKR represents a promising target for the development of novel anti-biofilm therapies due to its crucial role in regulating biofilm formation. Recent studies have shown that small molecules can effectively inhibit TCSs like GraSR, which are involved in antibiotic resistance mechanisms.[43] Similarly, targeting DesKR could provide a broad-spectrum approach to disrupting biofilm-associated infections and enhancing the efficacy of existing antibiotics against *S. aureus*. Future research should focus on elucidating the molecular structure of DesKR, identifying specific binding sites for small-molecule inhibitors, and employing in silico and structure-based drug design approaches.[44,45] Developing therapies targeting DesKR could significantly impact the treatment of biofilm-related infections and offer substantial clinical benefits.

Our study had certain limitations. Although our research indicated that *desKR* can regulate the expression of the *ica* operon, thereby affecting biofilm formation, further studies are required to confirm whether this regulatory effect is direct or indirect. Understanding the regulatory cascade that links *desKR* to PIA synthesis could provide valuable insights into the complex network of factors that control biofilm formation in *S. aureus* and may reveal new targets for anti-biofilm therapies. Further investigation of the molecular mechanisms underlying *desKR*-mediated resistance to cell-wall-targeting antibiotics is of great clinical significance.

In conclusion, our study demonstrates that the *desKR* two-component system is a key regulator of antibiotic resistance, adhesion, colonization and biofilm formation in *S. aureus* (Figure 7). The lineage-dependent distribution of *desKR* highlights the importance of considering strain-specific differences when studying the pathogenesis and antibiotic resistance of this important human pathogen. Our findings not only contribute to a better understanding of the molecular mechanisms governing biofilm formation in *S. aureus* but also identify *desKR* as a potential target for the development of novel strategies to combat biofilm-related infections. Future research should focus on elucidating the precise molecular mechanisms by which *desKR* regulates its downstream targets, and exploring the potential of targeting this two-component system for the prevention and treatment of *S. aureus* infections.

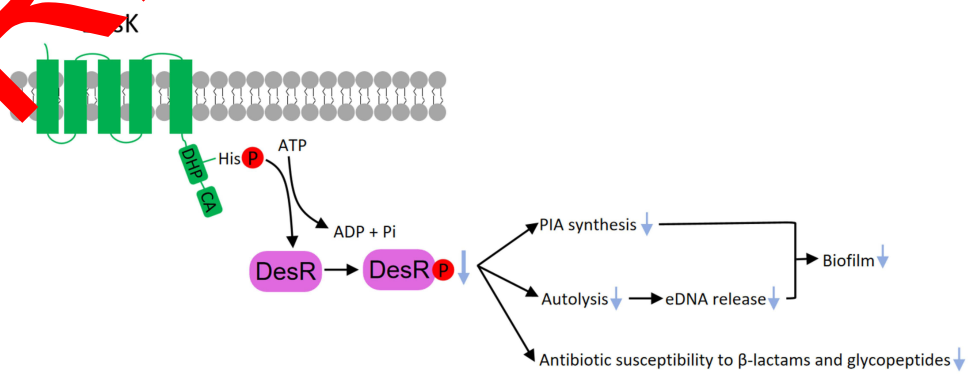

Figure 7 Schematic overview of the *S. aurues* DesKR two-component system and its regulatory effects on biofilm formation and antibiotic susceptibility.

Abbreviations

CLSM, Confocal laser scanning microscopy; MIC, minimum inhibitory concentration; MLST, multilocus sequence typing; NCBI, National Center for Biotechnology Information; STs, sequence type; SMART, Simple Modular Architecture Research Tool; CFU: Colony-forming units; CLSM, Confocal Laser Scanning Microscopy; PIA, polysaccharide intercellular adhesin; eDNA, extracellular DNA; TSBG, Tryptic Soy Broth containing 0.5% glucose; RT-qPCR, Real-time quantitative PCR.

Ethics Statement

All animal experiments were approved by the Animal Welfare and Ethics Committees of Yangzhou University and complied with the Ethics Committee of Laboratory Animals and guidelines of the Institutional Administrative Committee (SYXK 2022-0044).

Funding

This research was funded by grants from the Chinese National Science Foundation Grants (N[illegible]. 31972708, 31502075, 31873010, and 31672579), supported by the 111 Project D18007, and the Project Funded by the Priority Academic Program Development of Jiangsu Higher Education Institutions.

Disclosure

The authors declare no conflicts of interest in this work.

References

1. Tong SYC, Davis JS, Eichenberger E, Holland TL, Fowler VG. *Staphylococcus aureus* infections: epidemiology, pathophysiology, clinical manifestations, and management. *Clin Microbiol Rev*. 2015;283:603–661. doi:10.1128/CMR.00134-14
2. Idrees M, Sawant S, Karodia N, Rahman A. *Staphylococcus aureus* biofilm: morphology, genetics, pathogenesis and treatment strategies. *Int J Environ Res Public Health*. 2021;18:7602. doi:10.3390/ijerph18147602
3. Shree P, Singh CK, Sodhi KK, Surya JN, Singh DK. Biofilms: understanding structure and contribution towards bacterial resistance in antibiotics. *Med Microecol*. 2023;16:100084. doi:10.1016/j.medmic.2023.100084
4. Burgui S, Gil C, Solano C, Lasa I, Valle J. A systematic evaluation of the two-component systems network reveals that ArlRS is a key regulator of catheter colonization by *Staphylococcus aureus*. *Front Microbiol*. 2018;9. doi:10.3389/fmicb.2018.00342
5. Haag AF, Bagnoli F. The role of two-component signal transduction systems in *Staphylococcus aureus* virulence regulation. *Curr Top Microbiol Immunol*. 2017;409:145–198. doi:10.1007/82_2015_5019
6. Shaw C, Hess M, Weimer BC. Two-component systems and their role in bacterial virulence in response to the host gastrointestinal environment and metabolic cues. *Virulence*. 2022;13:1666–1686. doi:10.1080/21505594.2022.2127196
7. Ishii E, Eguchi Y. Diversity in sensing and signaling of bacterial sensor histidine kinases. *Biomolecules*. 2021;11:1524. doi:10.3390/biom11101524
8. Bhate MP, Molnar KS, Goulian M, DeGrado WF. Signal transduction in histidine kinases: insights from new structures. *Structure*. 2015;23(6):981–94. doi:10.1016/j.str.2015.04.002
9. Buelow DR, Raivio TL. Three (and more) component regulatory systems – auxiliary regulators of bacterial histidine kinases. *Mol Microbiol*. 2010;75:547–566. doi:10.1111/j.1365-2958.2009.06982.x
10. Kawada-Matsuo M, Yoshida Y, Nakamura N, Komatsuzawa H. Role of two-component systems in the resistance of *Staphylococcus aureus* to antibacterial agents. *Virulence*. 2011;2:427–430. doi:10.4161/viru.2.5.17711
11. Boles BR, Horswill AR. Agr-mediated Dispersal of *Staphylococcus aureus* Biofilms. *PLOS Pathog*. 2008;4:e1000052. doi:10.1371/journal.ppat.1000052
12. Toledo-Arana A, Merino N, Vergara-Irigaray M, Débarbouillé M, Penadés JR, Lasa I, Merino N, Vergara-Irigaray M Staphylococcus aureus develops an alternative, ica- Independent biofilm in the absence of the arlRS two-component system. *J Bacteriol*. 2005;187(15):5318–5329. doi:10.1128/JB.187.15.5318-5329.2005
13. Cue D, Junecko JM, Lei MG, et al. SaeRS-dependent inhibition of biofilm formation in *Staphylococcus aureus* Newman. *PLoS One*. 2015;10(4):e0123027. doi:10.1371/journal.pone.0123027
14. Dufresne K, DiMaggio DA, Maduta CS, Brinsmade SR, McCormick JK. Discovery of an antivirulence compound that targets the *Staphylococcus aureus* SaeRS two-component system to inhibit toxic shock syndrome toxin-1 production. *J Biol Chem*. 2024;300(7):107455. doi:10.1016/j.jbc.2024.107455
15. Gómez-Arrebola C, Hernandez SB, Culp EJ, et al. *Staphylococcus aureus* susceptibility to complestatin and corbomycin depends on the VraSR two-component system. *Microbiol Spectr*. 2023;11(5):e0037023. doi:10.1128/spectrum.00370-23
16. Fernández P, Díaz AR, Ré MF, et al. Identification of novel thermosensors in gram-positive pathogens. *Front Mol Biosci*. 2020;7:592747. doi:10.3389/fmolb.2020.592747
17. Enright MC, Day NP, Davies CE, Peacock SJ, Spratt BG. Multilocus sequence typing for characterization of methicillin-resistant and methicillin-susceptible clones of *Staphylococcus aureus*. *J Clin Microbiol*. 2000;38(3):1008–1015. doi:10.1128/JCM.38.3.1008-1015.2000
18. Monk IR, Shah IM, Xu M, Tan M-W, Foster TJ. Transforming the untransformable: application of direct transformation to manipulate genetically *Staphylococcus aureus* and *Staphylococcus epidermidis*. *mBio*. 2012;3:e00277–11. doi:10.1128/mBio.00277-11
19. Novick R. Properties of a cryptic high-frequency transducing phage in *Staphylococcus aureus*. *Virology*. 1967;33(1):155–166. doi:10.1016/0042-6822(67)90105-5

20. I S, H C, S C. Draft genome sequence of methicillin-sensitive *Staphylococcus aureus* ATCC 29213. *Genome Announc*. 2015;3: 10–128. doi:10.1128/genomeA.01095-15
21. MacLea KS, Trachtenberg AM. Complete genome sequence of *Staphylococcus epidermidis* ATCC 12228 chromosome and plasmids, generated by long-read sequencing. *Genome Announc*. 2017;5(36):e00954–17. doi:10.1128/genomeA.00954-17
22. Bae T, Schneewind O. Allelic replacement in *Staphylococcus aureus* with inducible counter-selection. *Plasmid*. 2006;55(1):58–63. doi:10.1016/j.plasmid.2005.05.005
23. Lee CY, Buranen SL, Ye ZH. Construction of single-copy integration vectors for *Staphylococcus aureus*. *Gene*. 1991;103(1):101–105. doi:10.1016/0378-1119(91)90399-V
24. Jolley KA, Bray JE, Maiden MCJ. Open-access bacterial population genomics: bIGSdb software, the PubMLST.org website and their applications. *Wellcome Open Res*. 2018;3:124. doi:10.12688/wellcomeopenres.14826.1
25. Letunic I, Khedkar S, Bork P. SMART: recent updates, new developments and status in 2020. *Nucleic Acids Res*. 2021;49(D1):D458–D460. doi:10.1093/nar/gkaa937
26. Waterhouse A, Bertoni M, Bienert S, et al. Swiss-MODEL: homology modelling of protein structures and complexes. *Nucleic Acids Res*. 2018;46(W1):W296–W303. doi:10.1093/nar/gky427
27. Gilchrist CLM, Chooi Y-H. clinker & clustermap.js: automatic generation of gene cluster comparison figures. *Bioinforma Oxf Engl*. 2021;37(16):2473–2475. doi:10.1093/bioinformatics/btab007
28. Balamurugan P, Praveen Krishna V, Bharath D, et al. *Staphylococcus aureus* quorum regulator SarA targeted compound, 2-[(M[illegible]hylamino)methyl] phenol inhibits biofilm and down-regulates virulence genes. *Front Microbiol*. 2017;8:1290. doi:10.3389/fmic[illegible]017.01290
29. Dotto C, Lombarte Serrat A, Cattelan N, et al. The active component of aspirin, salicylic acid, promote[illegible]*taphyl*[illegible]*ccus aureu*[illegible]iofilm formation in a PIA-dependent manner. *Front Microbiol*. 2017;8(4). doi:10.3389/fmicb.2017.00004.
30. Schlag S, Nerz C, Birkenstock TA, Altenberend F, Götz F. Inhibition of staphylococcal biof[illegible] formati[illegible] by nit[illegible] *Bacteriol*. 2007;189(21):7911–7919. doi:10.1128/JB.00598-07
31. Xi H, Luo Z, Liu M-F, et al. Diclofenac sodium effectively inhibits the biofilm formation of *[illegible]aphyl*[illegible]*s epiderm*[illegible]*s*. *Arch Microbiol*. 2024;206(7):289. doi:10.1007/s00203-024-04020-5
32. Rice KC, Mann EE, Endres JL, et al. The cidA murein hydrolase regulator contribute[illegible]A release and[illegible]m development in *Staphylococcus aureus*. *Proc Natl Acad Sci U S A*. 2007;104(19):8113–8118. doi:10.1073/pnas.06[illegible]226104
33. Yu G, Xi H, Sheng T, et al. Sub-inhibitory concentrations of tetrabromobisphenol A indu[illegible] the biofilm formation of methicillin-resistant *Staphylococcus aureus*. *Arch Microbiol*. 2024;206(7):301. doi:10.1007/s00[illegible]02-04022-3
34. Livak KJ, Schmittgen TD. Analysis of relative gene expression data u[illegible]ng real-time quantitative PCR and the 2(-Delta Delta C(T)) Method. *Methods San Diego Calif*. 2001;25(4):402–408. doi:10.1006/meth.2001.[illegible]62
35. Grundmann H, Aires-de-Sousa M, Boyce J, Tiemersma E. Emergen[illegible] and resurgen[illegible] of meticillin-resistant *Staphylococcus aureus* as a public-health threat. *Lancet*. 2006;368(9538):874–885. doi:10.1016/S0140[illegible]36(06)688[illegible]3
36. Stock AM, Robinson VL, Goudreau PN. Two-component [illegible] transductio[illegible] *Rev Biochem*. 2000;69(1):183–215. doi:10.1146/annurev.biochem.69.1.183
37. Bleul L, Francois P, Wolz C. Two-component systems of *S. [illegible]ureus*[illegible] and sensing mechanisms. *Genes*. 2021;13(34):34. doi:10.3390/genes13010034
38. Gardete S, Wu SW, Gill S, Tomasz A. Role of VraSR in antibiotic resistance and antibiotic-induced stress response in *Staphylococcus aureus*. *Antimicrob Agents Chemother*. 2006;50(10):[illegible]24–3434. doi:10.112[illegible]AAC.00356-06
39. Fernandes PB, Reed P, Monteiro JM, Pinho[illegible]G. Revis[illegible] role of VraTSR in *Staphylococcus aureus* response to cell wall-targeting antibiotics. *J Bacteriol*. 2022;204:e00162–22. doi:[illegible]1128[illegible]00162-22
40. Howden BP, McEvoy CRE, Allen [illegible], et al. Evo[illegible]ion of multidrug resistance during *Staphylococcus aureus* infection involves mutation of the essential two component regulat[illegible]KR. *PLoS Pa[illegible]g*. 2011;7(11):e1002359. doi:10.1371/journal.ppat.1002359
41. Verhoeven PO, Gagnaire J, B[illegible]elho-N[illegible]rs E, et al. Detection and clinical relevance of *Staphylococcus aureus* nasal carriage: an update. *Expert Rev Anti Infect Ther*. 2014;12(1):75–89. d[illegible]10.1586/14787210.2014.859985
42. Kranjec C, Morales Ar[illegible]es D, Torrissen M[illegible]i M, et al. Staphylococcal biofilms: challenges and novel therapeutic perspectives. *Antibiot Basel Switz*. 2021;10:131[illegible]:10.3390/antibiotics10020131
43. Dhankhar P, Dalal [illegible] Kotra[illegible]G, Kumar P. i In-silico approach to identify novel potent inhibitors against GraR ofi *S. aureus*i. *Front Biosci Landmark Ed*. 2020;[illegible]37–1360[illegible]i:10.2741/4859
44. Dalal V, D[illegible]r P, Si[illegible]V, et al. Structure-based identification of potential drugs against FmtA of *Staphylococcus aureus*: virtual screening, molecul[illegible]dynam[illegible], MM-G[illegible]SA and QM/MM. *Protein J*. 2021;40(2):148–165. doi:10.1007/s10930-020-09953-6
45. Kum[illegible]R, Dalal[illegible]. Identificati[illegible]n of potential inhibitors for LLM of *Staphylococcus aureus*: structure-based pharmacophore modeling, molecular dynam[illegible]and[illegible]nergy studies. *J Biomol Struct Dyn*. 2022;40(20):9833–9847. doi:10.1080/07391102.2021.1936179